doi:10.4149/neo_2021_210810N1132

Liver X receptors agonist T0901317 exerts ferroptosis sensitization in cancer

Meng-Ting ZHOU[1,#], Zhen-Yu LI[1,#], Jun FAN[2], Pin-Dong LI[1], Ye WANG[1], Sheng ZHANG[1,*], Xiao-Fang DAI[1,*]

[1]*Cancer Center, Union Hospital, Tongji Medical College, Huazhong University of Science and Technology, Wuhan, China;* [2]*Department of Pathology, Union Hospital, Tongji Medical College, Huazhong University of Science and Technology, Wuhan, China*

**Correspondence: tonydppx@hotmail.com; 2003xh1047@hust.edu.cn*
[#]Contributed equally to this work.

Received August 10, 2021 / Accepted December 6, 2021

Numerous studies have confirmed the anticancer effects of ferroptosis on a wide range of tumors, specifically in providing new perspectives for tackling drug resistance and treating refractory tumors. Notably, mechanisms of improving tumor susceptibility to ferroptosis have been a focus of current research. This study discovered that co-treatment of LXRS agonist T0901317 and ferroptosis inducers (FINs) significantly inhibited the proliferation of cancer cells, this inhibition effect could be reversed by specific inhibitors of ferroptosis and accompanied by elevated lipid peroxides. Glutathione peroxidase 4 (GPX4) regulates T0901317 induced ferroptotic sensitization, and its overexpression dramatically reverses the joint anticancer effect of T0901317 and FINs. Furthermore, xenograft model results highly confirmed the ferroptotic sensitization effect of T0901317 *in vivo*. In summary, our findings indicate that drug combination and ferroptosis induction strategies provide novel options for cancer therapy.

Key words: liver X receptors, ferroptosis, agonist, sensitivity, drug combination

Exploring novel methods of cell death has been a focal aspect of oncology research, geared towards providing new ideas for resolving refractory tumors and drug resistance. Apoptosis is the most prevalent form of programmed death during the development and treatment of cancer [1]. However, escaping apoptosis is a major hallmark of cancer, which potentially induces drug resistance [2, 3]. Ferroptosis is a form of programmed cell death with unique morphological and biochemical characteristics, whose induction is characterized by iron-dependent lipid peroxidation [4]. Cancer cells escaping apoptosis may keep or gain vulnerability to ferroptosis. System Xc^- and glutathione peroxidase 4 (GPX4) play a critical regulatory function in ferroptotic cell death [4–6]. System Xc^- regulates the uptake of cystine whereas intracellular cystine is an indispensable component of glutathione synthesis [7, 8]. Of note, GPX4 catalyzes reduced glutathione into oxidized form while reducing phospholipid hydroperoxides to non-toxic phospholipid alcohols, hence protecting lecithin-containing biofilms from lipid peroxidation attack [9]. The most representative ferroptosis inducers (FINs) stimulate ferroptosis by inhibiting System Xc^- or GPX4.

Ferroptosis is closely related to the development of benign diseases including ischemia-reperfusion injury, atherosclerosis, and neurodegeneration as well as involved in suppression of tumors. Several lines of evidence show that FINs exhibit favorable tumor-suppressive effects in *in vivo* and *in vitro* experiments [8–11]. Despite ferroptosis-specific agonists introducing new opportunities for cancer therapy, numerous challenges remain to be addressed before these agents are applied to clinical therapy. The intake of these agents potentially causes damage to normal tissues by ferroptosis during cancer therapy. Besides, long-term use of these drugs possibly causes or aggravates atherosclerosis, neurodegenerative disease, and diabetes [12–15]. Therefore, we sought to identify a ferroptotic sensitizer that can alleviate normal tissue damage by limiting the dose of ferroptosis inducers while enhancing the anti-tumor effect through a combination of drugs.

Liver X receptors (LXRS) are crucial members of the ligand-activated nuclear receptors (NRs) transcription factor superfamily. Due to their roles in regulating cholesterol and fatty acid metabolism, they are typically used as potential targets in the treatment of cardiovascular disorders [16–18]. T0901317 is a widely used LXRS agonist with studies reporting that it inhibits the growth of many cancers including liver cancer, gastric cancer, colon cancer, and breast cancer *in vitro* and *in vivo* [19–21]. Also, LXRS facilitates the synthesis of polyunsaturated fatty acid (PUFA) by

promoting the transcription of related genes [22]. Considering that PUFA is necessary for lipid peroxidation and ferroptosis, we speculate that LXRS agonists might act as a ferroptotic sensitizer.

To investigate whether LXRS sensitizes cancer cells to ferroptosis, cytotoxicity, and cell proliferation, experiments were performed to evaluate the presence of a joint anti-tumor effect of T0901317 and ferroptosis inducers Eratin/RSL3 and a correlation between this effect and ferroptosis. Moreover, we conducted flow cytometry to measure changes in ferroptosis-specific lipid peroxides under different treatment conditions. Eventually, a tumor-bearing model was applied to further validate the joint effect of co-treatment of Erastin and T0901317 *in vivo*. In summary, our study provides a potential strategy for cancer treatment via a combination of drugs based on ferroptotic cell death.

Materials and methods

Reagents. Compounds used in the experiment included Erastin (S7242, Selleckchem, Houston, TX, USA), RSL3 (S8155, Selleckchem, Houston, TX, USA), T0901317 (S7076, Selleckchem, Houston, TX, USA), Ferrostatin-1 (S7243, Selleckchem, Houston, TX, USA), Deferiprone (S4067, Selleckchem, Houston, TX, USA), Z-VAD-FMK (S7023, Selleckchem, Houston, TX, USA), Necrostatin-1 (S4157, Selleckchem, Houston, TX, USA), C11 BIODIPY 581/591 (D3681, Thermo Fisher, Waltham, MA, USA), Propidium Iodide (ST511, Beyotime, Shanghai, China), Cell Counting Kit-8 (C0037, Beyotime, Shanghai, China), anti-GPX4 antibody (ab125066, Abcam, Cambridge, UK), anti-beta-Tubulin antibody (ab6046, Abcam, Cambridge, UK), anti-Ki67 antibody (9449, Cell Signaling).

Cell culture. HCT116, Calu-1, and H1299 were cultured in RPMI-1640/Dulbecco's modified Eagle's medium (DMEM) supplemented with 10% fetal bovine serum (FBS) and 1% penicillin/streptomycin in a humid environment at 37 °C with 5% CO_2. The culture medium was changed and cells were passaged every day.

Cell proliferation and cell viability assay. Cell viability assay was implemented using the CCK-8 method. Cells were trypsinized, resuspended, and seeded in 96-well plates at 5–10×10^4/ml. After overnight incubation, cells were treated with different agents for 24 h. Cell viability was measured using Cell Counting Kit-8 following the manufacturer's instructions. The absorption values of wells were detected using a multifunctional microplate reader (Bio-Rad Laboratories, Hercules, CA, USA). Cell proliferation was evaluated via a clone formation experiment. Cells were seeded in 6-well plates at 1000/well, and after overnight incubation, they were treated with different agents for 24 h. The culture medium was changed every day, and after 7–10 days, the medium was removed and cells were fixed with 10% methanol. After washing with phosphate-buffered saline (PBS), the cells were stained using a 1% crystal violet solution.

Flow cytometry. Lipid peroxidation *in vitro* was detected using a lipid ROS probe; cells were treated with defined drugs for 24 h, then incubated with 2 μmol C11 BODIPY 581/591 (D3681, Thermo Fisher, Waltham, MA, USA) for 30 min. To remove residual C11 BODIPY 581/591, cells were washed using PBS. Thereafter, cells were trypsinized and resuspended in PBS. Lipid ROS generated in cells oxidized the dye causing a shift of the fluorescence emission peak from ~590 nm to ~510 nm, which was positively correlated with the mean fluorescence value detected by flow cytometry.

PI staining was used in detecting the proportion of dead cells. Cells were seeded and treated as above-mentioned. After 24 h, the supernatants were separately collected from each well and transferred into a centrifuge tube. The cells were rinsed twice with pre-warmed PBS, and 0.5 ml of pre-warmed trypsin was added to each well. The cells were then neutralized with the previously collected supernatant after trypsinization. After centrifugation, the supernatant was discarded, and cells were resuspended in 500 μl PBS. Exactly 10 μl PI stock solution (1 mg/ml) was added to each tube, and the percentage of PI-positive cells in each group was analyzed by flow cytometry after 10 min of incubation at room temperature.

Western blot analysis. Cells were lysed using RIPA buffer and collected in a centrifuge tube and left on ice for 30 min. The supernatant was extracted after centrifugation (12,000×g, 20 min, 4 °C). A loading buffer was added after protein quantification and placed in a thermostat water bath (100 °C, 10 min). After electrophoresis, the bands were transferred to polyvinylidene fluoride (PVDF) transfer membrane. Then, the membranes were blocked with 5% skimmed milk prepared in TBST solution for 1 h under ambient conditions. Thereafter, the membranes were incubated in diluted primary antibody buffer overnight at 4 °C. After washing, the membranes were further incubated with diluted secondary antibody solution for 1 h. Visualization of bands was performed using the chemiluminescence kit and ImageJ (National Institutes of Health) was used for the analysis of results.

Transfection of GPX4 expressing lentivirus. Lentivirus transfection: Calu-1 cells were plated in a 6-well plate 5×10^4 cells/well. On the next day, when adherent and in good condition, they were rinsed with PBS. 1 ml complete medium and 5 μl polybrene were added to each well for the pretreatment. After 2 h, 5 μl GPX4-expressing lentivirus and corresponding vector lentivirus were added to the wells respectively. After 24 h, the supernatant was changed and 1 ml of a medium was added to each well.

Screening of cells: After 48 h, the cells grew to 60–70% confluence and were in good condition. The supernatant was removed and rinsed using PBS. Exactly 2.5 μg/ml of puromycin-containing medium was added to continue the culture. Intracellular green fluorescence was visible under a fluorescence microscope.

Validation: The cell line was validated at RNA or protein level via PCR and western blot. After successful verification,

part of the cells was expanded and frozen while others were cultured for subsequent experiments.

Xenograft model. Four-week-old female BALB/c nu/nu (13–15 g) mice were purchased. The rearing of the mice was reviewed and approved by the Ethics Committee of Tongji Medical College of Huazhong University of Science and Technology. After the mice were adapted to the environment, the transplantation tumor model was constructed. 1×10^7 HCT116 cells were injected into the right shoulder and back of the mouse. Drug treatment was performed when the average tumor volume reached 100 mm^3, mice were randomly divided into 4 groups, i.e., 1) vehicle group, 2) RSL3 group, 3) T0901317 group, and 4) RSL3 plus T0901317 group. Drugs were administered via intraperitoneal injection. RSL3 and T0901317 doses were 50 mg/kg each, and the control group was administered with a similar volume of a drug solvent. The body weight and tumor volume were measured at intervals of three days after the start of treatment (V = long diameter × short $diameter^2/2$). After 15 days, mice were humanely sacrificed, tumor tissue was stripped and weighed, then stored in paraformaldehyde for subsequent experiments.

Statistical analysis. The t-test was performed using GraphPad Prism 7.0 (GraphPad, CA, USA) to analyze the data. A p-value <0.05 indicated a statistical significance.

Results

T0901317 inhibited the proliferation of cancer cells. To establish the effect of T0901317 on the activity of tumor cells, Calu-1, H1299, and HCT-116 cells were treated with different concentrations of T0901317 (1–50 μmol). After 24 hours of treatment, cell viability experiments demonstrated an increased inhibitory effect of drugs on cancer cells with increasing drug concentration (Figures 1A–1C). Additionally, the pretreatment of ferroptosis inhibitor Ferrostatin-1 (1 μmol) could not reverse the above suppressing activity of T0901317 (Figures 1A–1C). These results indicated that T0901317 hinders the proliferation of cancer cells in a ferroptosis-independent manner.

The combination of T0901317 and ferroptosis inducers synergistically inhibited the proliferation of cancer cells. To display the synergistic effects of T0901317 and ferroptosis inducers (FINs) on the viability of cancer cells, cell viability and colony-forming assays were conducted. Calu-1, H1299, and HCT116 cells were treated with a low concentration of T0901317 (10 μmol) plus an increasing amount of Erastin (1–40 μmol)/RSL3 (0.005–1 μmol), notably, the single drug Erastin/RSL3 group was regarded as the control group. After 24 hours of treatment, T0901317 and Erastin/RSL3 had a combined inhibitory effect on the above 3 cancer cell lines. Meanwhile, the above treatments did not significantly inhibit the non-cancerous BEAS-2B cells (Figures 2A–D, Supplementary Figure S1). Colony-forming assay results showed that the co-treatment of T0901317 and ferroptosis agonists tremendously suppressed the clone efficiency of Calu-1 and H1299 cells, (Figures 2E–G). Besides, combined treatment reduced colony-forming efficiency (56±4% and 6±3%) compared to the single-use of FINs (103±6% and 88±5%). Collectively, these findings suggested that T0901317 improves the inhibitory action of ferroptosis inducers on cancer cells.

T0901317 sensitized cancer cells to ferroptosis. Based on biochemical and morphological characteristics, cell death can be subdivided into several types including apoptosis, ferroptosis, necroptosis, and so forth. To determine the mechanism of the synergistic cytotoxic effects of T0901317 and Erastin/RSL3, Calu-1, H1299, and HCT-116 cells were divided into the control group (DMSO), Erastin (10 μmol) or RSL3 single-agent group, T0901317 (10 μmol) single-agent group and drug combination group. Each group was separately pretreated with DMSO, Deferoxamine (50 μmol), Ferrostatin-1 (1 μmol), Z-VAD-FMK (10 μmol), Necrostatin-1 (20 μmol). After 24 hours, cell viability assay confirmed that combination treatment exhibited stronger inhibition on cancer cells compared to the single-agent group,

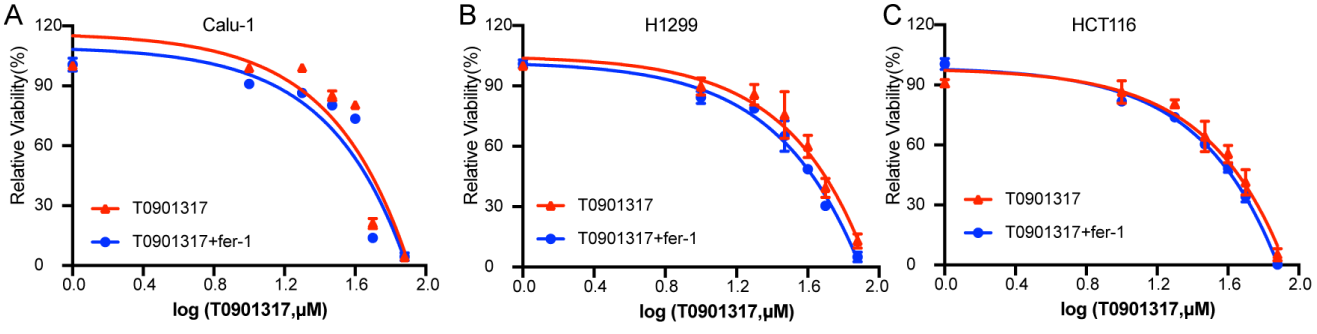

Figure 1. T0901317 inhibits the proliferation of cancer cells. A–C) Cell viability assay results for Calu-1, H1299, and HCT116 cells treated with growing concentrations of T0901317 (1–50 μmol) alone or with the pretreatment of 1 μmol Ferrostatin-1 (fer-1) for 24 h. Error bars are means ± SD from three independent samples.

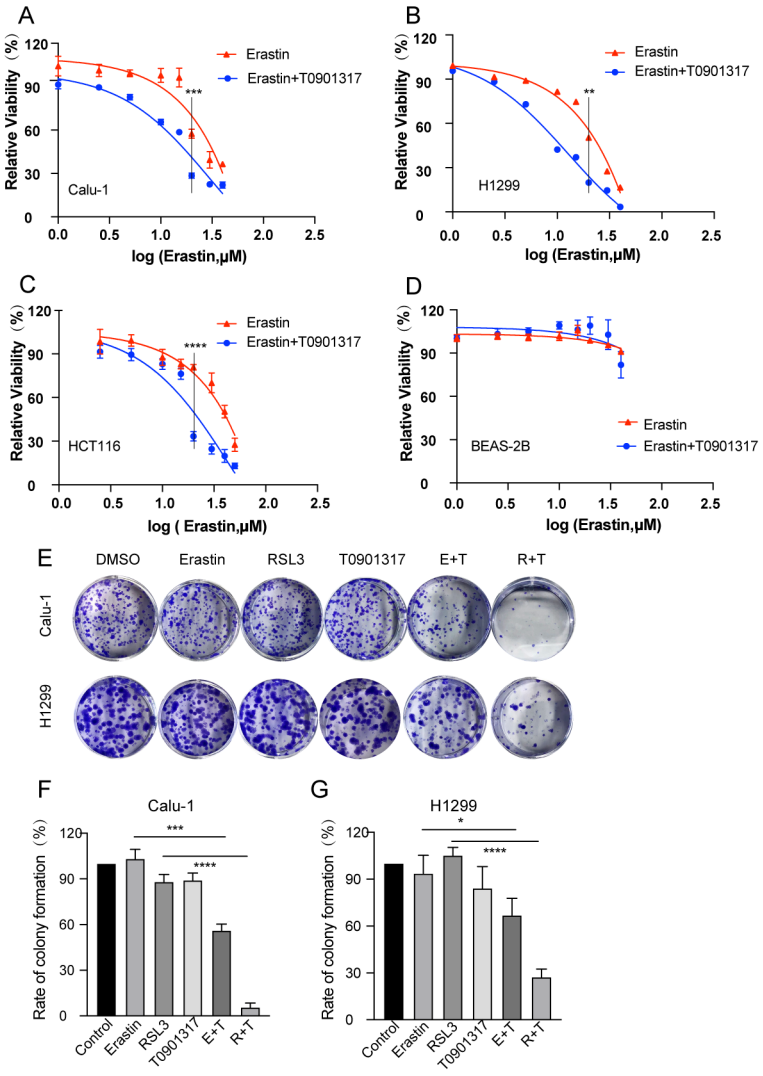

Figure 2. T0901317 and FINs in combination synergistically reduce the viability of cancer cells. A–D) Low concentrations of T0901317 (10 μmol) significantly elevated the cytotoxic effect of Erastin on Calu-1, H1299, and HCT116, while the same treatment did not exhibit a discernible suppressive effect on BEAS-2B. Error bars are means ± SD from three independent samples. E) Emblematic images of colony formation experiments in Calu-1 and H1299 cells that were exposed to different agents. (F–G) The calculated survival rate in colony formation assays in Calu-1 and H1299. Error bars are means ± SD from three independent samples. *p<0.05; **p<0.01; ***p<0.001; ****p<0.0001, two-tailed unpaired Student's t-test.

with the survival rate of Calu-1 decreasing from 76±4% and 77±3% to 31±2% and 9±2%. The above suppression effect could be blunted by specific inhibitors of ferroptosis-Deferoxamine and Ferrostatin-1, yet apoptosis inhibitor Z-VAD-FMK could not reverse the synergistic antitumor effect. Also, necroptosis inhibitor Necrostatin-1 abolished the decrease in cell activity in the combined group (Figures 3A–F), notably, previous reports indicated the compound function as a non-specific ferroptosis inhibitor [23].

Further, PI single-staining flow cytometry was performed on the above-mentioned groups to confirm the role of T0901317 in ferroptotic sensitization. At the concentrations of T0901317 and FINs assessed, either single agent only induced a slight increase in the proportion of PI-positive cells. The proportion of PI staining positive cells caused by a combined treatment was significantly higher compared to that by the monotherapy. Pretreatment with Deferoxamine (50 μmol) and Ferrostatin-1 (1 μmol) significantly counteracted the above synergistic inhibitory effect (Figures 3G–I). Collectively, T0901317 could not elicit ferroptosis in cancer but enhanced the sensitivity of cancer to ferroptosis.

T0901317 enhances FINs-induced lipid peroxidation. Lipid peroxidation is an important hallmark and a key step in ferroptosis [6]. C11 BODIPY 581/591 is a probe used for detecting lipid-derived active oxygen. The fluorescence intensity is proportional to the content of lipid-derived active

oxygen. To investigate the co-treatment effect of T0901317 and Erastin/RSL3 on lipid peroxidation, Calu-1, H1299, and HCT116 were grouped based on different treatment conditions. As a consequence, there was a significant enhancement in fluorescence intensity under the co-treatment of T0901317 and FINs compared to T0901317 or FINs treatment alone. Deferoxamine and Ferrostatin-1 effectively suppressed lipid peroxidation caused by the above-mentioned treatments (Figures 4A–B), indicating a synergistic antitumor effect of T0901317 via ferroptosis sensitization.

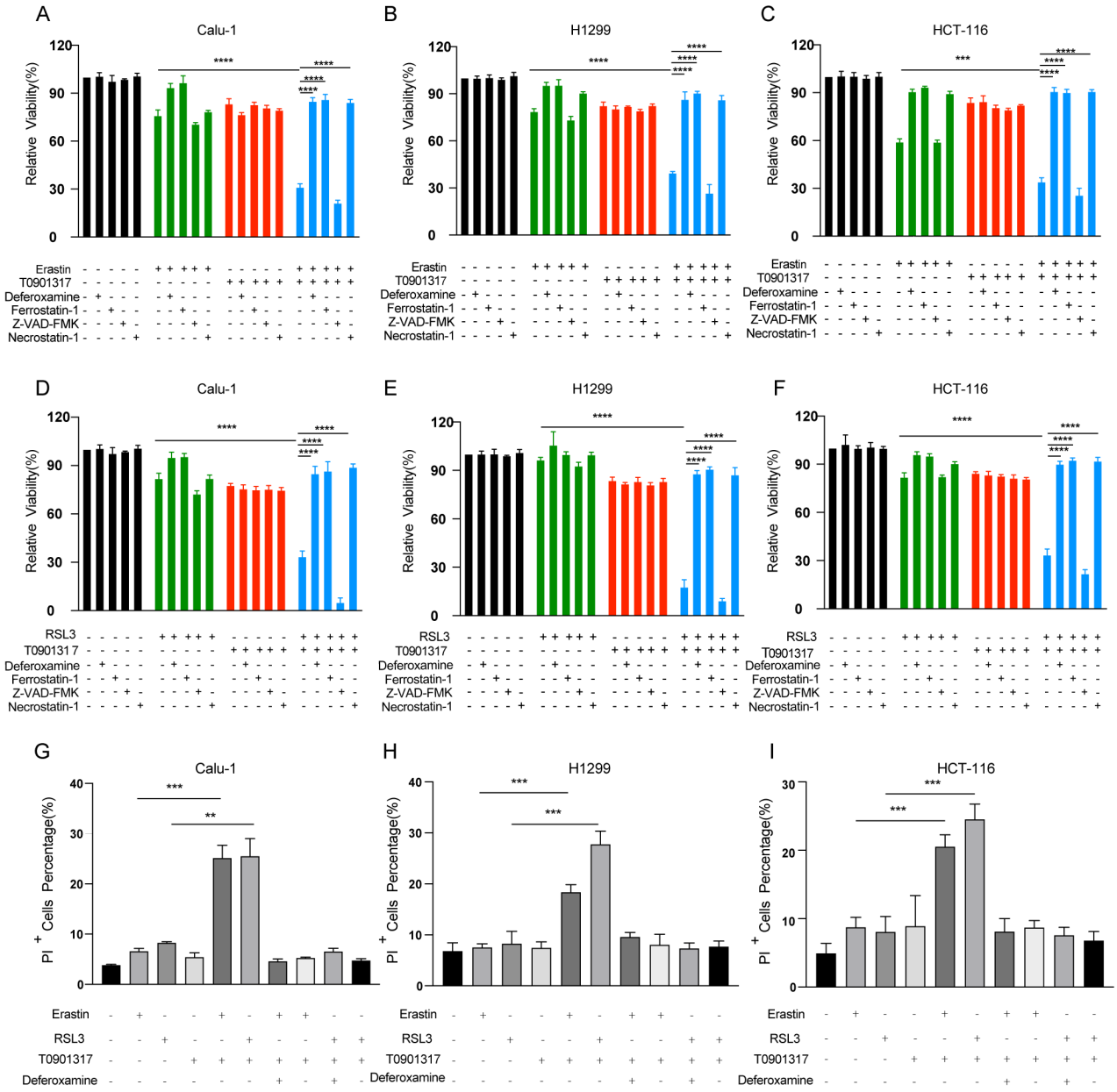

Figure 3. T0901317 sensitizes cancer cells to ferroptosis. A–C) Cells were treated with Erastin, T0901317, or Erastin+T0901317 (E+T) in the absence or presence of Deferoxamine (50 μmol), Ferrostatin-1 (1 μmol), Z-VAD-FMK (10 μmol), or Necronstatin-1 (20 μmol). Cell viability assays were conducted after treatment for 24 h. Error bars are means ± SD from three independent samples. *p<0.05; **p<0.01; ***p<0.001; ****p<0.0001, two-tailed unpaired Student's t-test. D–F) Cells were treated with RSL3, T0901317, or RSL3+T0901317 (R+T) in the absence or presence of Deferoxamine (50 μmol), Ferrostatin-1 (1 μmol), Z-VAD-FMK (10 μmol), or Necronstatin-1 (20 μmol). Cell viability assays were conducted after treatment for 24 h. Error bars are means ± SD from three independent samples. *p<0.05; **p<0.01; ***p<0.001; ****p<0.0001, two-tailed unpaired Student's t-test. G–I) PI staining was evaluated by flow cytometry for the quantification of dead cells. Error bars are means ± SD from three independent samples. *p<0.05; **p<0.01; ***p<0.001; ****p<0.0001, two-tailed unpaired Student's t-test.

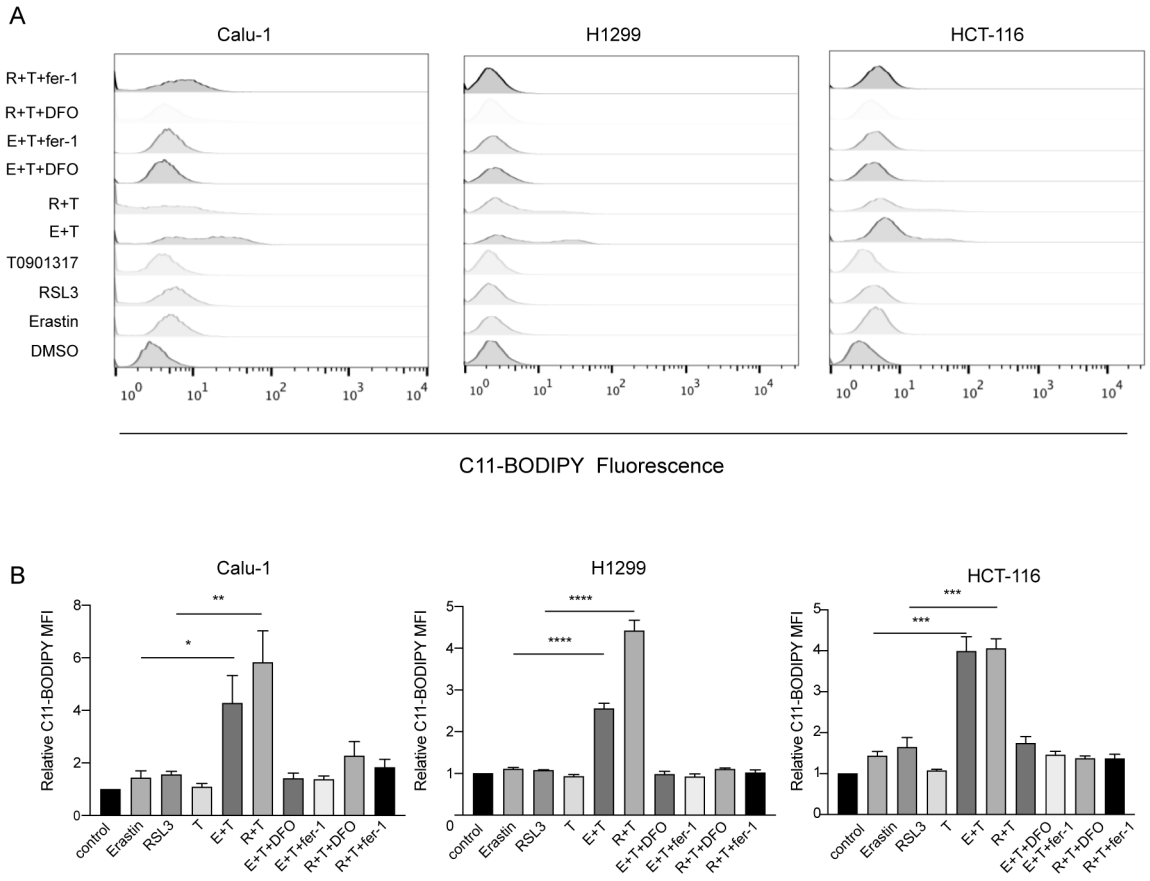

Figure 4. T0901317 enhances FINs-induced lipid peroxidation. A) Evaluation of lipid peroxidation by C11 BODIPY probe in Calu-1, H1299, and HCT116 cell lines after exposed to the indicated treatment for 24 h. B) Relative mean florescence intensity values of C11 BODIPY are shown, *p<0.05; **p<0.01; ***p<0.001; ****p<0.0001, two-tailed unpaired Student's t-test.

GPX4 plays an important part in T0901317 induced ferroptosis sensitization. A total of two most prevalent mechanisms have been reported in ferroptosis induction, one is by inhibiting System Xc^- while the other is by inhibiting glutathione peroxidase 4 (GPX4) [4, 9]. β-mercaptoethanol serves as a ferroptosis inhibitor by increasing cystine intake while Ebselen acts as glutathione peroxidase mimic protects cells from GPX4 inhibition [4, 5, 24]. The results of the cell viability assay showed that β-mercaptoethanol only mildly saved H1299 cells from drug combination inhibition, however, Ebselen remarkably rescued cells from joint suppression (Figure 5A). We preliminarily speculated that T0901317 exerts ferroptosis sensitization through synergistic inhibition of GPX4. Western blot results revealed that the expression of GPX4 under T0901317 alone treatment had no significant change, its markedly decreased under the co-treatment of T0901317 and Erastin/RSL3 (Figure 5B).

To further confirm this conjecture, a GPX4-overexpressing Calu-1 cell line was constructed and verified at protein and mRNA expression levels (Figures 5C, 5D). Calu-1 and GPX4-overexpressing Calu-1 cells were separately subdivided into 4 groups, i.e., control (DMSO), RSL3 (0.025 μmol), T0901317 (10 μmol), and RSL3+T0901317 groups. After 24 h, a depressed density and morphological changes of cells induced by the combined treatment were observed compared to those administrated by monotherapy in Calu-1 cells via microscope. However, under a similar co-treatment condition, GPX4-overexpressing Calu-1 cells were in good condition and favorable cell viability versus those in Calu-1 cells (Figures 5E–F). Also, colony formation experiments confirmed the afore-mentioned findings, i.e., GPX4 overexpression conspicuously impaired joint inhibition in H1299 cells (Figure 5G). In summary, GPX4 regulates T0901317-mediated ferroptosis sensitization.

T0901317 and RSL3 joint inhibited tumor growth *in vivo*. According to previous findings in *in vitro* experiments, this study further explored whether T0901317 and RSL3 had a synergistic antitumor effect on HCT-116 loaded xenograft models. Unsurprisingly, the growth rate of tumor volume and tumor weight in mice administered with T0901317 and/or RSL3 were lower compared to that received drug solvent and joint treatment with much better inhibitory effects on

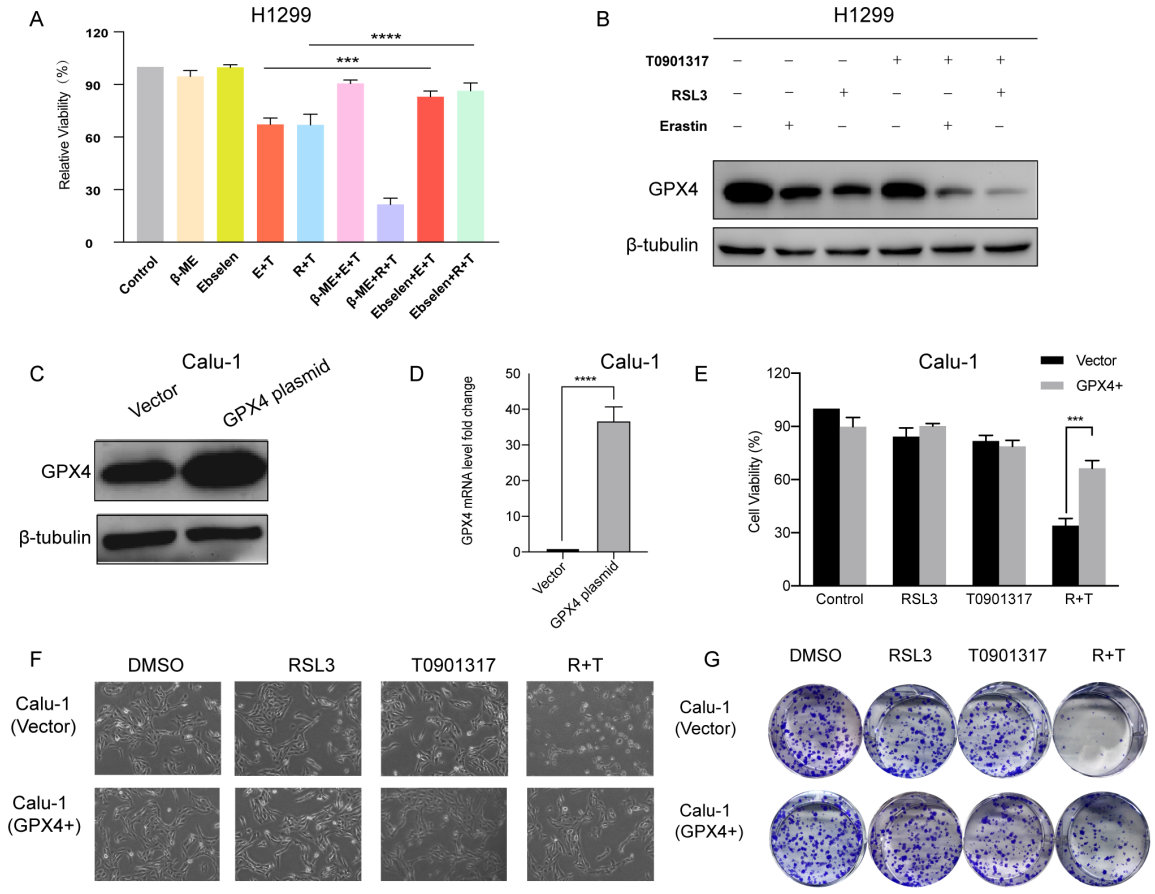

Figure 5. GPX4 plays an important part in T0901317-induced ferroptosis sensitization. A) Cell viability assay of H1299 cells exposed to different treatment conditions. B) Western blot representative images analysis of GPX4 expression changes in H1299 cells under indicated treatment. C, D) Validation of GPX4 overexpression in Calu-1 cells. Vector or GPX4 overexpression Calu-1 cells were exposed to indicated treatment, representative pictures observed under a microscope, quantification of cell survival and images of colony formation (E–G) are shown. *p<0.05; **p<0.01; ***p<0.001; ****p<0.0001, two-tailed unpaired Student's t-test.

tumor growth versus either single agent (Figures 6A–C). Additionally, no difference in weight was noted between groups (Figure 6D), indicating low toxicity *in vivo*. Tumor tissue H&E staining results showed more dead cells in the co-treatment group compared to those in the monotherapy group (Figure 6E). Less proportion of Ki-67 and GPX4 stained positive cells were discovered in the combined group compared to the single-agent group (Figure 6E). By validating previous findings of *in vitro* experiments, our *in vivo* results indicated that T0901317 could sensitize cancer to ferroptosis.

Discussion

Liver X receptors (LXRS) are a type of nuclear receptors (NRs). Since they regulate lipid and cholesterol metabolism, LXRS are critical targets in the research of diseases including atherosclerosis and diabetes. Notably, their activation in experiments dramatically inhibits the progression of these diseases [16, 25]. Additionally, LXRS exert anti-tumor functions through transcriptional modulation of biological processes involving cell cycle, inflammatory responses, and lipid metabolism, qualifying them as essential targets for cancer research [26–28]. T0901317, a widely used agonist of LXRS was experimentally found to suppress colon cancer, gastric cancer, and prostate cancer [19–21]. Herein, we identified that T0901317 itself could not directly induce ferroptosis in cancer, whereas it enhanced the cytotoxicity of ferroptosis inducers on cancer. The aforementioned sensitization can be inhibited by ferroptosis-specific inhibitors accompanied by an increase in lipid peroxidation level. Moreover, T0901317 combined with ferroptosis elicitors significantly lowered the expression of GPX4 in cancer, and to a large extent, overexpression of GPX4 could reverse the combination suppressive effect. The effect of the drug combination *in vivo* was further confirmed by the xenograft model. In summary, T0901317

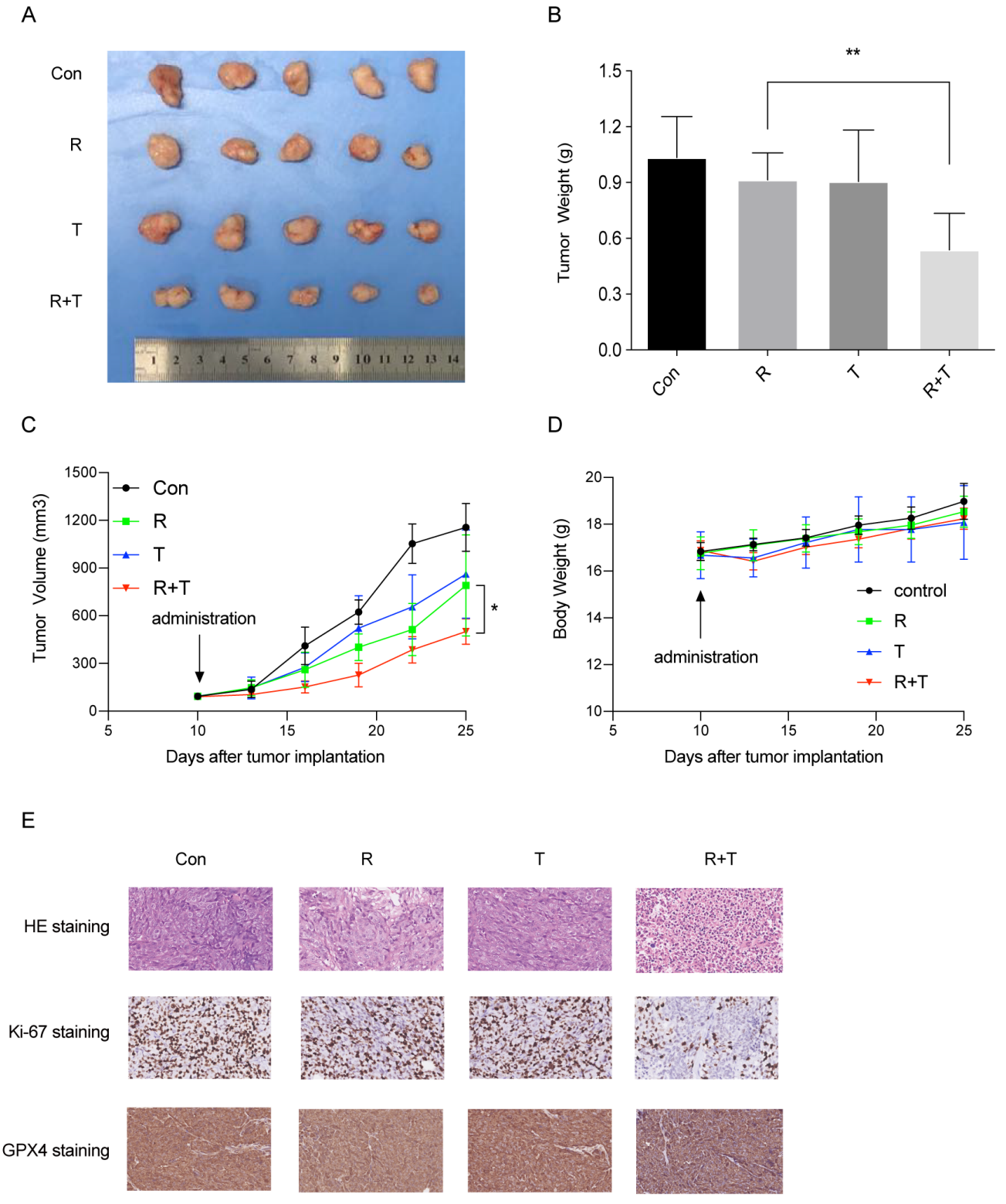

Figure 6. T0901317 and RSL3 jointly inhibit tumor growth *in vivo*. HCT116 cells-xenograft model was built in BALB/c nude mice, then treated them with RSL3 (50 mg/kg), T0901317 (50 mg/kg), or the combination of both for 15 days. Tumor images (A) and tumor weights (B) are shown, *p<0.05; **p<0.01; ***p<0.001; ****p<0.0001, two-tailed unpaired Student's t-test. Changes of tumor volume (C) and body weight (D) were monitored, *p<0.05; **p<0.01; ***p<0.001; ****p<0.0001, paired Student's t-test. E) H&E staining and immunohistochemistry staining for Ki-67 and GPX4 in tumor tissue.

exerts ferroptosis sensitizing effects in cancer by synergistically suppressing the expression of GPX4.

The emergence of ferroptosis introduces novel options for overcoming tumor resistance and treating refractory tumors. Recent studies revealed that highly mesenchymal state cancer cells with metastatic potential are therapeutically resistant to conventional chemotherapy and targeted therapy, yet such cells are extremely susceptible to GPX4-specific inhibitors [29]. The existence of persister cancer cells (PCCs) has been highly associated with multidrug resistance. Besides, the highly mesenchymal state of PCCs renders it more sensitive to GPX4 suppression compared to its parental counterparts. *In vivo* experiments showed that knocking out GPX4 significantly reduced the probability of cancer recurrence after targeted therapy [30]. GPX4 expression was higher in tumor tissues than in normal tissues, and there was a negative correlation between GPX4 expression in tumor tissues and the prognosis of patients [31]. In addition, the expression level of the cystine glutamate reverse transporter SLC7A11 in tumor tissues was negatively associated with chemotherapy sensitivity [32]. Therefore, ferroptosis is a promising new and effective therapeutic approach in cancer. Also, GPX4 and System Xc^- are potential targets for cancer therapy. Although ferroptosis-specific inhibitors are promising in the treatment of cancer, many challenges remain to be surmounted before these inhibitors are applied in the preclinical and clinical settings. For instance, consistent and intensive intake of ferroptosis inhibitors might cause or exacerbate iron metabolic disorders including atherosclerosis, myocardial dysfunction, diabetes, and neurodegenerative diseases [12–15]. As such, the search for an effective ferroptosis sensitizer provides a practical idea for overcoming the above-mentioned challenges.

Despite ferroptosis-specific inducers are not being applied in the clinical treatment of cancer, ferroptosis promotes therapeutic interventions in several major types of cancer. For instance, a previous study revealed that radiotherapy induces ferroptosis by activating ataxia-telangiectasia mutated gene to inhibit SLC7A11. The induction of ferroptosis by radiotherapy was further substantiated by another study. Radiation stimulated lipid peroxidation and ferroptosis by producing reactive oxygen species and upregulating the expression of Acyl Coenzyme A Synthetase Long-Chain Family, Member 4 (ACSL4) [33, 34]. Also, ferroptosis is implicated in the antitumor effects caused by immunotherapy, and IFNγ produced by immunotherapy-activated CD8+ T cells inhibits solute carrier family 7 member 11 (SLC7A11) causing lipid peroxidation and ferroptosis in cancer [35]. Notably, a few agents including cisplatin, sulfasalazine, statins, and sorafenib approved by the Food and Drug Administration have been identified to induce cancer ferroptosis *in vitro* and *in vivo* [29, 36–38]. Therefore, based on the drug combination strategy, our research provides a reference for optimizing the existing treatment regimens of cancer while lowering the systemic cytotoxicity by reducing the dose of drugs.

Supplementary information is available in the online version of the paper.

Acknowledgments: This work was financially supported by grants from the National Natural Science Foundation of China (NO. 81470108).

References

[1] HASSED C. A matter of life and death. Aust Fam Physician 2002; 31: 469–472.

[2] HANAHAN D, WEINBERG RA. Hallmarks of cancer: the next generation. Cell 2011; 144: 646–674. https://doi.org/10.1016/j.cell.2011.02.013

[3] IGNEY FH, KRAMMER PH. Death and anti-death: tumour resistance to apoptosis. Nat Rev Cancer 2002; 2: 277–288. https://doi.org/10.1038/nrc776

[4] DIXON SJ, LEMBERG KM, LAMPRECHT MR, SKOUTA R, ZAITSEV EM et al. Ferroptosis: an iron-dependent form of nonapoptotic cell death. Cell 2012; 149: 1060–1072. https://doi.org/10.1016/j.cell.2012.03.042

[5] XIE Y, HOU W, SONG X, YU Y, HUANG J et al. Ferroptosis: process and function. Cell Death Differ 2016; 23: 369–379. https://doi.org/10.1038/cdd.2015.158

[6] YANG WS, STOCKWELL BR. Ferroptosis: Death by Lipid Peroxidation. Trends Cell Biol 2016; 26: 165–176. https://doi.org/10.1016/j.tcb.2015.10.014

[7] KOPPULA P, ZHANG Y, ZHUANG L, GAN B. Amino acid transporter SLC7A11/xCT at the crossroads of regulating redox homeostasis and nutrient dependency of cancer. Cancer Commun (Lond) 2018; 38: 12. https://doi.org/10.1186/s40880-018-0288-x

[8] STOCKWELL BR, FRIEDMANN ANGELI JP, BAYIR H, BUSH AI, CONRAD M, et al. Ferroptosis: A Regulated Cell Death Nexus Linking Metabolism, Redox Biology, and Disease. Cell 2017; 171: 273–285. https://doi.org/10.1016/j.cell.2017.09.021

[9] YANG WS, SRIRAMARATNAM R, WELSCH ME, SHIMADA K, SKOUTA R et al. Regulation of ferroptotic cancer cell death by GPX4. Cell 2014; 156: 317–331. https://doi.org/10.1016/j.cell.2013.12.010

[10] GUINEY SJ, ADLARD PA, BUSH AI, FINKELSTEIN DI, AYTON S. Ferroptosis and cell death mechanisms in Parkinson's disease. Neurochem Int 2017; 104: 34–48. https://doi.org/10.1016/j.neuint.2017.01.004

[11] BASULI D, TESFAY L, DENG Z, PAUL B, YAMAMOTO Y et al. Iron addiction: a novel therapeutic target in ovarian cancer. Oncogene 2017; 36: 4089–4099. https://doi.org/10.1038/onc.2017.11

[12] CHEN GQ, BENTHANI FA, WU J, LIANG D, BIAN ZX et al. Artemisinin compounds sensitize cancer cells to ferroptosis by regulating iron homeostasis. Cell Death Differ 2020; 27: 242–254. https://doi.org/10.1038/s41418-019-0352-3

[13] HUANG J, JONES D, LUO B, SANDERSON M, SOTO J et al. Iron overload and diabetes risk: a shift from glucose to Fatty Acid oxidation and increased hepatic glucose production in a mouse model of hereditary hemochromatosis. Diabetes 2011; 60: 80–87. https://doi.org/10.2337/db10-0593

[14] HARE D, AYTON S, BUSH A, LEI P. A delicate balance: Iron metabolism and diseases of the brain. Front Aging Neurosci 2013; 5: 34. https://doi.org/10.3389/fnagi.2013.00034
[15] DABBAGH AJ, SHWAERY GT, KEANEY JF JR, FREI B. Effect of iron overload and iron deficiency on atherosclerosis in the hypercholesterolemic rabbit. Arterioscler Thromb Vasc Biol 1997; 17: 2638–2645. https://doi.org/10.1161/01.atv.17.11.2638
[16] IM SS, OSBORNE TF. Liver x receptors in atherosclerosis and inflammation. Circ Res 2011; 108: 996–1001. https://doi.org/10.1161/CIRCRESAHA.110.226878
[17] ZHANG Y, BREEVOORT SR, ANGDISEN J, FU M, SCHMIDT DR et al. Liver LXRalpha expression is crucial for whole body cholesterol homeostasis and reverse cholesterol transport in mice. J Clin Invest 2012; 122: 1688–1699. https://doi.org/10.1172/JCI59817
[18] JAKOBSSON T, TREUTER E, GUSTAFSSON JA, STEFFENSEN KR. Liver X receptor biology and pharmacology: new pathways, challenges and opportunities. Trends Pharmacol Sci 2012; 33: 394–404. https://doi.org/10.1016/j.tips.2012.03.013
[19] DERANGÈRE V, CHEVRIAUX A, COURTAUT F, BRUCHARD M, BERGER H et al. Liver X receptor β activation induces pyroptosis of human and murine colon cancer cells. Cell Death Differ 2014; 21: 1914–1924. https://doi.org/10.1038/cdd.2014.117
[20] WANG Q, FENG F, WANG J, REN M, SHI Z et al. Liver X receptor activation reduces gastric cancer cell proliferation by suppressing Wnt signalling via LXRβ relocalization. J Cell Mol Med 2019; 23: 789–797. https://doi.org/10.1111/jcmm.13974
[21] CHUU CP, KOKONTIS JM, HIIPAKKA RA, LIAO S. Modulation of liver X receptor signaling as novel therapy for prostate cancer. J Biomed Sci 2007; 14: 543–553. https://doi.org/10.1007/s11373-007-9160-8
[22] DEMEURE O, LECERF F, DUBY C, DESERT C, DUCHEIX S et al. Regulation of LPCAT3 by LXR. Gene 2011; 470: 7–11. https://doi.org/10.1016/j.gene.2010.09.002
[23] FRIEDMANN ANGELI JP, SCHNEIDER M, PRONETH B, TYURINA YY, TYURIN VA et al. Inactivation of the ferroptosis regulator Gpx4 triggers acute renal failure in mice. Nat Cell Biol 2014; 16: 1180–1191. https://doi.org/10.1038/ncb3064
[24] SCHEWE T. Molecular actions of ebselen--an antiinflammatory antioxidant. Gen Pharmacol 1995; 26: 1153–1169. https://doi.org/10.1016/0306-3623(95)00003-j
[25] HAYASHI T, KOTANI H, YAMAGUCHI T, TAGUCHI K, IIDA M et al. Endothelial cellular senescence is inhibited by liver X receptor activation with an additional mechanism for its atheroprotection in diabetes. Proc Natl Acad Sci U S A 2014; 111: 1168–1173. https://doi.org/10.1073/pnas.1322153111
[26] PANAGIOTAKOS DB, PITSAVOS C, POLYCHRONOPOULOS E, CHRYSOHOOU C, MENOTTI A et al. Total cholesterol and body mass index in relation to 40-year cancer mortality (the Corfu cohort of the seven countries study). Cancer Epidemiol Biomarkers Prev 2005; 14: 1797–1801. https://doi.org/.1158/1055-9965.Epi-04-0907
[27] VEDIN LL, LEWANDOWSKI SA, PARINI P, GUSTAFSSON JA, STEFFENSEN KR. The oxysterol receptor LXR inhibits proliferation of human breast cancer cells. Carcinogenesis 2009; 30: 575–579. https://doi.org/10.1093/carcin/bgp029
[28] KIM GH, PARK K, YEOM SY, LEE KJ, KIM G et al. Characterization of ASC-2 as an antiatherogenic transcriptional coactivator of liver X receptors in macrophages. Mol Endocrinol 2009; 23: 966–974. https://doi.org/10.1210/me.2008-0308
[29] VISWANATHAN VS, RYAN MJ, DHRUV HD, GILL S, EICHHOFF OM et al. Dependency of a therapy-resistant state of cancer cells on a lipid peroxidase pathway. Nature 2017; 547: 453–457. https://doi.org/10.1038/nature23007
[30] HANGAUER MJ, VISWANATHAN VS, RYAN MJ, BOLE D, EATON JK et al. Drug-tolerant persister cancer cells are vulnerable to GPX4 inhibition. Nature 2017; 551: 247–250. https://doi.org/10.1038/nature24297
[31] ZHANG X, SUI S, WANG L, LI H, ZHANG L et al. Inhibition of tumor propellant glutathione peroxidase 4 induces ferroptosis in cancer cells and enhances anticancer effect of cisplatin. J Cell Physiol 2020; 235: 3425–3437. https://doi.org/10.1002/jcp.29232
[32] HUANG Y, DAI Z, BARBACIORU C, SADÉE W. Cystine-glutamate transporter SLC7A11 in cancer chemosensitivity and chemoresistance. Cancer Res 2005; 65: 7446–7454. https://doi.org/10.1158/0008-5472.Can-04-4267
[33] LANG X, GREEN MD, WANG W, YU J, CHOI JE et al. Radiotherapy and Immunotherapy Promote Tumoral Lipid Oxidation and Ferroptosis via Synergistic Repression of SLC7A11. Cancer Discov 2019; 9: 1673–1685. https://doi.org/10.1158/2159-8290.Cd-19-0338
[34] LEI G, ZHANG Y, KOPPULA P, LIU X, ZHANG J et al. The role of ferroptosis in ionizing radiation-induced cell death and tumor suppression. Cell Res 2020; 30:146–162. https://doi.org/10.1038/s41422-019-0263-3
[35] WANG W, GREEN M, CHOI JE, GIJÓN M, KENNEDY PD et al. CD8(+) T cells regulate tumour ferroptosis during cancer immunotherapy. Nature 2019; 569: 270–274. https://doi.org/10.1038/s41586-019-1170-y
[36] LACHAIER E, LOUANDRE C, GODIN C, SAIDAK Z, BAERT M et al. Sorafenib induces ferroptosis in human cancer cell lines originating from different solid tumors. Anticancer Res 2014; 34: 6417–6422.
[37] GUO J, XU B, HAN Q, ZHOU H, XIA Y et al. Ferroptosis: A Novel Anti-tumor Action for Cisplatin. Cancer Res Treat 2018; 50: 445–460. https://doi.org/10.4143/crt.2016.572
[38] YU H, YANG C, JIAN L, GUO S, CHEN R et al. Sulfasalazine-induced ferroptosis in breast cancer cells is reduced by the inhibitory effect of estrogen receptor on the transferrin receptor. Oncol Rep 2019; 42: 826–838. https://doi.org/10.3892/or.2019.7189

https://doi.org/10.4149/neo_2021_210810N1132

Liver X receptors agonist T0901317 exerts ferroptosis sensitization in cancer

Meng-Ting ZHOU[1,#], Zhen-Yu LI[1,#], Jun FAN[2], Pin-Dong LI[1], Ye WANG[1], Sheng ZHANG[1,*], Xiao-Fang DAI[1,*]

Supplementary Information

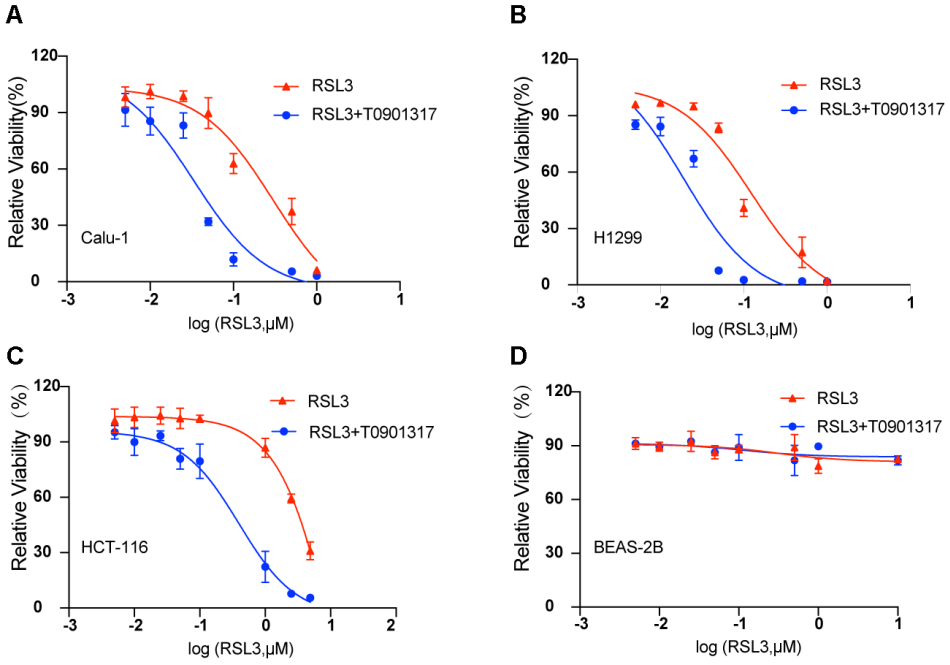

Supplementary Figure S1. Low concentrations of T0901317 (10 μmol) significantly elevated the cytotoxic effect of RSL3 on Calu-1 (A), H1299 (B), and HCT116 (C), while treatment did not exhibit a discernible suppressive effect on BEAS-2B (D). Error bars are means±SD from independent samples.